Theory of Sedimentation for Kinetically Controlled Dimerization Reactions†

John R. Cann* and Gerson Kegeles

ABSTRACT: Theoretical sedimentation patterns have been computed for reversible, kinetically controlled macromolecular dimerization reactions. Both nonmediated and ligand-mediated interactions have been examined over a range of conditions. The continuous transformation in the shape of the sedimentation pattern on passing from the limit of very rapid equilibration to the lower limit of negligibly slow equilibration has been followed. The patterns obtained for half-times of reaction as long as 20–60 sec are essentially the same as those for instantaneous reequilibration during differential transport of monomer and dimer. For half-times of dissociation of the dimer less than about 200 sec, resolution of the reaction boundary into two peaks can occur only if dimerization is ligand mediated. The bimodal patterns for rapidly equilibrating ligand-mediated dimerization may bear a strong resemblance to those shown by slowly equilibrating systems. The implications of these findings for detection and characterization of interacting systems by analytical sedimentation are discussed.

Ever since the pioneering work of Gilbert (1955) almost two decades ago there has been considerable interest in the sedimentation of reversibly associating macromolecules for which equilibration is rapid, but rather less attention has been paid to kinetically controlled association. The best understood of such interactions is the simple dimerization (reaction I)

$$2M \underset{k'_2}{\overset{k'_1}{\rightleftharpoons}} M_2 \qquad \text{(I)}$$

where k'_1 and k'_2 are the specific rates of reaction (primed to avoid subsequent duplication of symbols). For rates of reaction so fast that, in effect, there is local equilibrium between monomer, M, and dimer, M_2, during their differential transport, the sedimentation pattern will show a single peak (Gilbert, 1955, 1959). The unique feature of kinetically controlled dimerization is that the sedimentation pattern may show three peaks for half-times of reaction comparable to the time of sedimentation depending upon the values of other relevant parameters (Belford and Belford, 1963; Oberhauser *et al.*, 1965). Finally, for rates of reaction so slow that negligible interconversion occurs during the course of sedimentation, the pattern will show two peaks corresponding to separated monomer and dimer. Not all dimerization reactions, however, can be described as simply as in reaction I, some being mediated through the binding of small molecules or ions according to a scheme such as (reaction set II)

$$M + X \underset{k_2}{\overset{k_1}{\rightleftharpoons}} MX \qquad \text{(IIa)}$$

$$M + MX \underset{k_4}{\overset{k_3}{\rightleftharpoons}} M_2X \qquad \text{(IIb)}$$

in which X is a small ligand molecule. Although the theory of sedimentation for such ligand-mediated interactions is rather well understood for instantaneous establishment of equilibrium (Cann and Goad, 1972; Cann, 1970, 1973), prior to this investigation nothing was known about the sedimentation behavior when the reactions are kinetically controlled. Currently there is an awakening interest in kinetically controlled association reactions spurred by experimental observations on systems such as hemocyanin whose reversible dimerization is mediated by the binding of Ca^{2+} or Mg^{2+} and H^+. Thus, for example, in the case of hemocyanin from the New England lobster, *Homarus americanus*, equilibration is relatively rapid (Morimoto and Kegeles, 1971; Tai and Kegeles, 1971; Kegeles and Tai, 1973); while for hemocyanin from the Dungeness crab, *Cancer magister*, equilibration is slow (Ellerton *et al.*, 1970) perhaps due to the existence of two kinds of subunits (Carpenter and Van Holde, 1973).

In order to define as precisely as possible the effect of kinetic control on the shape of the sedimentation patterns for both nonmediated (reaction I) and ligand-mediated (reaction set II) dimerization, we have made the theoretical investigation reported below. The calculations are meant to simulate the sedimentation of hemocyanin under conditions such that the protein is about 50% dimerized,[1] but the results also apply qualitatively to proteins of lower molecular weight.

Theory

The theory to be described is for the moving-boundary mode of mass transport. Theoretical sedimentation patterns have been computed by numerical solution of the appropriate set of conservation equations which make the rectilinear and constant field approximations. Computations have been

† From the Department of Biophysics and Genetics, University of Colorado Medical Center, Denver, Colorado 80220, and the Section of Biochemistry and Biophysics U-125, The Biological Sciences Group, University of Connecticut, Storrs, Connecticut 06268. *Received November 7, 1973.* Supported in part by Research Grants 5 R01 HL 13909-22 and 5 R01 HL 13166-04 from the National Heart and Lung Institute, National Institutes of Health, U. S. Public Health Service. This publication is No. 569 from the Department of Biophysics and Genetics, University of Colorado Medical Center, Denver, Colo.

[1] Actually the dimerization of New England lobster hemocyanin is mediated by the binding of 4–6 Ca^{2+} and 2–4 H^+; but a kinetic scheme with multiple ligand binding is mathematically formidable. Inductive reasoning indicates that even though reaction set II assumes a single binding site, it makes an acceptable approximation to the real system when ligand binding proceeds very much more rapidly than dimerization. In the limit of instantaneous establishment of both equilibria, the chief discrepancy is in the range of unbound-ligand concentration over which bimodal reaction boundaries would be predicted for fixed per cent dimerization; the greater the number of binding sites, the higher the concentration at which resolution could still occur.

made both for kinetically controlled interactions and for the limiting case of rates of reaction so fast that, in effect, there is local equilibrium among the interacting species. In the case of kinetically controlled interactions quite different approaches were used for nonmediated and ligand-mediated dimerization, respectively; and each is considered separately below. The theory for ligand-mediated dimerization also illustrates the numerical procedure used for the forementioned limiting case of instantaneous reestablishment of equilibrium during differential transport of the several species.

Nonmediated Dimerization (Reaction I). It is assumed that during sedimentation of a macromolecule in solution it dimerizes reversibly with a specific rate constant k'_1, M^{-1} sec^{-1}, and that the dimer dissociates with a specific rate constant k'_2, sec^{-1}; where $k'_1/2k'_2 = K$, M^{-1}, is the dimerization constant. In the monomeric and dimeric states, M and M_2, the macromolecule migrates with sedimentation coefficients s_1 and s_2 and diffuses with diffusion coefficients D_1 and D_2. The changes in concentrations of M and M_2, C_1 and C_2 expressed in moles per liter, with time of sedimentation, t, and position in the sedimentation column, x, are described by the system of conservation equations

$$\partial C_1/\partial t = D_1(\partial^2 C_1/\partial x^2) - v_1(\partial C_1/\partial x) - k'_1 C_1^2 + 2k'_2 C_2 \quad (1a)$$

$$\partial C_2/\partial t = D_2(\partial^2 C_2/\partial x^2) - v_2(\partial C_2/\partial x) + (1/2)k'_1 C_1^2 - k'_2 C_2 \quad (1b)$$

where v_i ($i = 1, 2$) is the driven velocity. $v_i = s_i\omega^2\bar{x}$ in which $\omega^2\bar{x}$ is the constant field strength; ω, angular velocity; and $\bar{x}$, an average position. In our calculations, $\omega^2\bar{x} = 2.6056 \times 10^8$ cm sec^{-2} which corresponds to 60,000 rpm and $\bar{x} = 6.6$ cm. Equations 1a and 1b conserve mass by taking into account diffusion, transport in the centrifugal field, and chemical reaction. Their solution gives the sedimentation pattern of the reacting system. To this end we introduce the new position variable

$$x' = x - \bar{v}t \quad (2)$$

in which $\bar{v}$ is the average macromolecular velocity

$$\bar{v} = (v_1 + v_2)/2 \quad (3)$$

Equations 1a and 1b are transformed into the moving coordinate system simply by making the replacements

$$x' \longrightarrow x$$
$$v_i - \bar{v} \longrightarrow v_i$$

We now introduce discrete time and position variables

$$t_n = n\Delta t \quad n = 0, 1, 2, \ldots$$
$$x'_l = l\Delta x' \quad l = 0, 1, 2, \ldots, L$$

and replace the continuous variables $C_i(t,x')$ by the discrete variables $C_i(n\Delta t, l\Delta x') \equiv C_i(t_n, x'_l)$. Proceeding as in a previous investigation (Cann and Goad, 1965a), the transformed eq 1a is approximated by the finite difference equation

$$C_1(t_{n+1}, x'_l) = C_1(t_n, x'_l) + \frac{D_1\Delta t}{(\Delta x')^2}\{C_1(t_n,x'_{l+1}) - 2C_1(t_n,x'_l) + C_1(t_n,x'_{l-1})\} - \frac{(v_1 - \bar{v})\Delta t}{\Delta x'}\{C_1(t_n,x'_{l+1}) - C_1(t_n,x'_l)\} - k'_1\Delta t C_1^2(t_n,x'_l) + 2k'_2\Delta t C_2(t_n,x'_l) \quad (4a)$$

and similarly for eq 1b, taking care to use the forward difference in concentration when approximating the first spatial derivative. Given the values of C_i at any time t, we can calculate their values at $t + \Delta t$ using eq 4. Thus, given initial conditions and boundary values, recursive solution of these equations in time allows one to follow the evolution of the sedimentation pattern.

The initial conditions are

$$C_1(0,x'_l) = C_2(0,x'_l) = 0 \quad l = 0, 1, 2, \ldots, L/2$$
$$C_1(0,x'_l) = C_{10},\ C_2(0,x'_l) = KC_{10}^2 \equiv C_{20}$$
$$l = L/2 + 1, \ldots, L$$

which corresponds to a sharp boundary between a solution containing equilibrium concentrations of M and M_2 overlaid with solvent. The concentrations of M and M_2 in the initial equilibrium solution are designated as C_{10} and C_{20}, respectively.

The boundary values are

$$C_1(t_n,0) = C_2(t_n,0) = 0$$
$$C_1(t_n,x'_L) = C_{10}$$
$$C_2(t_n,x'_L) = KC^2_{10} \equiv C_{20}$$

Computations were made on the University of Colorado's CDC 6400 electronic computer. The values of $\Delta t = 1$ sec and $\Delta x' = 0.01$ cm used in these calculations satisfy the stability criterion employed previously (Cann and Goad, 1965a). The value of Δt was chosen so as to be more than an order of magnitude smaller than the shortest half-time of reaction considered.

In order to simulate the sedimentation of a 1.16% solution of hemocyanin under dimerizing conditions, the following values were assigned to the several parameters: $C_{10} + 2C_{20} = 2.326 \times 10^{-5}$ M; initial per cent dimerization, $100 \times 2C_{20}/(C_{10} + 2C_{20}) = 52.7\%$; $K = 5.067 \times 10^4$ M^{-1}; $s_1 = 17$ S and $s_2 = 25$ S. In the case of the diffusion coefficients, cognizance must be taken of the truncation error due to the way in which the first spatial derivatives in the transformed eq 1a and 1b are approximated in eq 4. This error expressed itself as excess spreading ("truncation diffusion") of the peaks in the sedimentation pattern, the solution of the difference equations corresponding closely to the solution of the differential equations in which the quantity

$$|v_i - \bar{v}|\Delta x'/2$$

has been added to the diffusion coefficients (Goad and Cann, 1969). In the present calculations the value of this quantity is 5.21×10^{-7} cm^2 sec^{-1}. If this were to be added to the physical values (about 3×10^{-7} cm^2 sec^{-1}) of the diffusion coefficients, the half-widths of the calculated peaks exclusive of spreading due to reaction would be about 70% greater than one would wish. This discrepancy was decreased to about 30% by the expediency of choosing values of D_1 and D_2 such that their sums with 5.21×10^{-7} give values (6.21×10^{-7} and 5.31×10^{-7} cm^2 sec^{-1}, respectively) for the mathematically effective diffusion coefficients which are in better agreement with the physical values for M and M_2.

Finally, we have explored a range of k'_2 values at constant K. In the limit of reaction rates so slow that virtually no interconversion occurs during sedimentation, the conservation equations for M and M_2 were uncoupled by deleting the chemical kinetic terms from the right hand side of eq 4.

The computed sedimentation patterns are displayed as plots of molar concentration gradient, $\delta(C_1 + 2C_2)/\delta x'$, against position, x'. Two vertical arrows indicate where the peaks in the patterns would have been located had sedimentation

been carried out on a mixture of noninteracting macromolecules having the same transport parameters as monomer and dimer.

Ligand-Mediated Dimerization (*Reaction Set II*). Theoretical sedimentation patterns for ligand-mediated dimerization have been computed by numerical solution of the set of transport equations for constituent macromolecule and constituent ligand. The salient features of the calculation are as follows. Suppose the sedimentation column to be divided into a number of discrete segments. Given the initial equilibrium concentrations of the several species in each segment, we calculate the change in the distribution of material during a short interval of time, Δt, due to transport. It is assumed that there is no reequilibration by interaction during Δt, each species migrating independently from its distribution at the beginning of the interval. After the concentrations have been advanced, equilibrium is recalculated. That is, for known constituent concentrations of macromolecule and ligand computed from the concentrations of the several species as changed by transport, new equilibrium concentrations are calculated by applying the law of mass action. At this juncture the calculation can be carried in either of two directions depending upon the rates of reaction.

(1) If the computations are for the limiting case of *instantaneous reestablishment of equilibrium* during differential transport of the several species, we simply compute the change in the newly equilibrated distribution of material due to transport over the next Δt; recalculate the equilibrium; and so on, constructing the entire evolution of the distribution of material in the sedimentation column from the initial condition.

(2) For *kinetically controlled* interactions, we proceed by first relaxing the concentrations for a length of time equal to Δt from their values as changed by transport toward their new equilibrium values using the theory of relaxation kinetics (Eigen and DeMaeyer, 1963). The concentrations in each segment as changed by reaction then constitute the starting distribution of material for the next time cycle of transport which is followed, in turn, by relaxation of ligand binding; relaxation of the dimerization reaction; and so on, again constructing the evolution of the distribution of material in the sedimentation column from the initial condition. The numerical procedure is sketched below.[2]

In contrast to nonmediated dimerization, there are four sedimenting species in the case of the ligand-mediated reaction (M, MX, M_2X, and X); and the simplifying assumptions are made that both monomeric species, M and MX, have the same diffusion and sedimentation coefficients and that the sedimentation coefficient of unbound ligand, X, is zero. The molar concentrations of the macromolecular species are designated as $C_{i,k}$, where $i = 1$ or 2 designates monomer or dimer and $k = 0$ or 1 designates the number of bound ligand molecules (*e.g.*, $C_{2,1}$ is the concentration of the dimer, M_2X). Their transport parameters bear the subscript i. The molar concentration and diffusion coefficient of unbound ligand are designated as C_3 and D_3, respectively.

The conservation equations for independent transport of the four species in the moving coordinate system specified by eq 2 and 3,

$$\partial C_{i,k}/\partial t = D_i(\partial^2 C_{i,k}/\partial x'^2) - (v_i - \bar{v})(\partial C_{i,k}/\partial x') \qquad i = 1, 2;\ k = 0, 1$$

$$\partial C_3/\partial t = D_3(\partial^2 C_3/\partial x'^2) + \bar{v}(\partial C_3/\partial x')$$

are approximated by finite difference equations as described above for the case of nonmediated dimerization. Given values of $C_{i,k}$ and C_3 at any time T, we calculate their values at $t + \Delta t$ as changed by transport using the finite difference equations. For sake of clarity the values of the concentrations as changed by transport will be designated as $\hat{C}_{i,k}$ and $\hat{C}_3$.

At each time, t_{n+1}, new values of the constituent concentrations of macromolecule, $\bar{C}_M$, and ligand, $\bar{C}_X$, are computed from $\hat{C}_{i,k}$ and $\hat{C}_3$

$$\bar{C}_M = \hat{C}_{1,0} + \hat{C}_{1,1} + 2\hat{C}_{2,1}$$

$$\bar{C}_X = \hat{C}_3 + \hat{C}_{1,1} + \hat{C}_{2,1}$$

and then equilibration is imposed by simultaneous solution of the mass action expressions

$$\bar{C}_M = C_{1,0} + K_1C_{1,0}C_3 + 2K_1K_2C_{1,0}^2C_3 \qquad (5a)$$

$$\bar{C}_X = C_3 + K_1C_{1,0}C_3 + K_1K_2C_{1,0}^2C_3 \qquad (5b)$$

for the equilibrium values of $C_{1,0}$ and C_3 (designated for clarity as $\bar{C}_{1,0}$ and $\bar{C}_3$) which, in turn, are used to calculate the equilibrium values

$$\bar{C}_{1,1} = K_1\bar{C}_{1,0}\bar{C}_3$$

$$\bar{C}_{2,1} = (1/2)(\bar{C}_M - \bar{C}_{1,0} - \bar{C}_{1,1})$$

In these equations $K_1 = k_1/k_2$, M^{-1}, is the equilibrium constant for binding of ligand to M (reaction IIa); $K_2 = k_3/k_4$, M^{-1}, the dimerization constant (reaction IIb); and the specific rate constants k_1 and k_3 have the dimensions, M^{-1} sec^{-1}, and k_2 and k_4, sec^{-1}. To solve eq 5a and 5b we apply the Newton–Raphson method (Carnahen *et al.*, 1969), using the values of $C_{1,0}$ and C_3 at time t_n as starting approximations except when either of these is zero in which case 0.5 $\bar{C}_M$ or 0.5 $\bar{C}_X$ is used. If the computations are for *instantaneous reestablishment of equilibrium* during differential transport, these new values of the equilibrium concentrations serve as the starting distribution of material for the next time cycle of transport followed by reequilibration; and so on, thereby following the evolution of the sedimentation pattern. If, on the other hand, the computations are for *kinetically controlled* interactions, the concentrations of the several species as changed by transport must first be relaxed toward their equilibrium values for a length of time equal to ΔT before proceeding to the next time cycle of transport.

Toward this end we apply the theory of relaxation kinetics as follows. (1) Calculate the displacements, $y_{i,k}^0$ and y_3^0, of the concentrations as changed by transport from their equilibrium values

$$y_{i,k}^0 = \bar{C}_{i,k} - \hat{C}_{i,k}$$

$$y_3^0 = \bar{C}_3 - \hat{C}_3$$

(2) Define the instantaneous values of the concentrations as

$$C_{i,k} = \bar{C}_{i,k} - y_{i,k} \qquad (6a)$$

[2] In principle the same numerical method used for reaction I could also be used for reaction set II; *i.e.*, the chemical kinetic terms could be incorporated directly into the conservation equations, in analogy with eq 1a,b. In practice, however, the computational time required becomes prohibitive. This is so because the value of Δt must be at least an order of magnitude less than the shortest half-time of reaction, which for rapidly equilibrating ligand binding (reaction IIa) is of the order of 10^{-4}–10^{-2} sec. Otherwise, the change in concentrations of the reacting species during each time cycle of calculation would be so large as to give a physically meaningless solution and would no doubt give rise to instability of the finite-difference equations. These difficulties are circumvented by the alternative numerical method using relaxation kinetics as described in the text for reaction set II.

$$C_3 = \bar{C}_3 - y_3 \tag{6b}$$

where $y_{i,k}$ and y_3 are the instantaneous displacements of the concentrations from their equilibrium values. (3) Formulate the rate equations for the change in concentrations with time, *e.g.*

$$dC_3/dt = -k_1C_{1,0}C_3 + k_2C_{1,1} \tag{7}$$

(4) Substitute eq 6a and 6b into eq 7 and linearize the rate equations by neglecting higher order terms in the y's thereby obtaining the set of simultaneous rate equations for the change in the y's with time

$$dy_3/dt = -k_1\bar{C}_3y_{1,0} + k_2y_{1,1} - k_1\bar{C}_{1,0}y_3 \tag{8a}$$

$$dy_{2,1}/dt = k_3\bar{C}_{1,1}y_{1,0} + k_3\bar{C}_{1,0}y_{1,1} - k_4y_{2,1} \tag{8b}$$

$$dy_{1,0}/dt + dy_{1,1}/dt + 2(dy_{2,1}/dt) = 0 \tag{8c}$$

$$dy_3/dt + dy_{1,1}/dt + dy_{2,1}/dt = 0 \tag{8d}$$

(5) Make the usual assumption that for small displacements from equilibrium

$$dy_{i,k}/dt = -y_{i,k}/\tau \tag{9a}$$

$$dy_3/dt = -y_3/\tau \tag{9b}$$

where τ is a relaxation time, and substitute eq 9a and 9b into eq 8a–d to obtain the system of homogeneous linear equations

$$-k_1\bar{C}_3y_{1,0} + k_2y_{1,1} - (k_1\bar{C}_{1,0} - 1/\tau)y_3 = 0$$

$$k_3\bar{C}_{1,1}y_{1,0} + k_3\bar{C}_{1,0}y_{1,1} - (k_4 - 1/\tau)y_{2,1} = 0$$

$$y_{1,0} + y_{1,1} + 2y_{2,1} = 0$$

$$y_3 + y_{1,1} + y_{2,1} = 0$$

whose determinant formed from the coefficients of the y's is zero for nontrivial solutions. Expansion of the determinant yields a quadratic equation in $1/\tau$ whose roots are the reciprocals of two relaxation times, τ_1 and τ_2 sec. The relaxation times are evaluated by taking the sum of the roots in order to eliminate the radical in the quadratic formula and their product to remove the radical sign over the discriminant. Since we assume that the ligand-binding reaction IIa equilibrates much more rapidly than the dimerization reaction IIb, $\tau_1 \ll \tau_2$ in which case we find that

$$1/\tau_1 = k_2[K_1(\bar{C}_{1,0} + \bar{C}_3) + 1]$$

$$\frac{1}{\tau_2} = k_4 + \frac{k_4K_2[2K_1\bar{C}_{1,0}\bar{C}_3 + 2\bar{C}_{1,1} + K_1\bar{C}_{1,0}(\bar{C}_{1,0} + \bar{C}_{1,1})]}{[K_1(\bar{C}_{1,0} + \bar{C}_3) + 1]}$$

(6) In words, the particular solutions of the system of eq 8 are exponential functions (expressed in differential form by eq 9a and 9b) which satisfy the equations for two different relaxation times. This means that the general solution is the sum of two exponential terms each multiplied by an integration constant. Thus, the general solution of eq 8 is

$$y_3 = A_3e^{-t/\tau_1} + B_3e^{-t/\tau_2} \tag{10a}$$

$$y_{2,1} = A_{2,1}e^{-t/\tau_1} + B_{2,1}e^{-t/\tau_2} \tag{10b}$$

where the integration constants A and B are evaluated from initial conditions, *e.g.*

$$A_3 = k_2(K_1\bar{C}_3y_{1,0}^0 - y_{1,1}^0 + K_1\bar{C}_{1,0}y_3^0 - y_3^0/k_2\tau_2)[(1/\tau_1) - (1/\tau_2)]^{-1}$$

$$B_3 = y_3^0 - A_3$$

In our numerical procedure we set $t = \Delta t$; calculate y_3 and $y_{2,1}$ using eq 10a and 10b; calculate $y_{1,1}$ from the conservation equation

$$y_{1,1} = -y_3 - y_{2,1} + y_3^0 + y_{2,1}^0 + y_{1,1}^0$$

and then calculate the concentrations as changed by reaction during the time Δt

$$C_3 = \bar{C}_3 - y_3$$

$$C_{2,1} = \bar{C}_{2,1} - y_{2,1}$$

$$C_{1,1} = \bar{C}_{1,1} - y_{1,1}$$

$$C_{1,0} = (\bar{C}_{1,0} + \bar{C}_{1,1} + 2\bar{C}_{2,1}) - C_{1,1} - 2C_{2,1}$$

These concentrations now constitute the starting distribution of material for the next time cycle of transport which is followed, in turn, by equilibration, relaxation, etc. Given initial conditions and boundary values this recursive calculation constructs the evolution of the sedimentation pattern.

The initial conditions are

$$C_{1,0}(0,x'_l) = C_{1,1}(0,x'_l) = C_{2,1}(0,x'_l) = C_3(0,x'_l) = 0 \qquad l = 0, 1, 2, \ldots, L/2$$

$$C_{1,0}(0,x'_l) = C_1^0/(1 + R),$$

$$C_{1,1}(0,x'_l) = C_1^0 - C_{1,0}(0,x'_l),$$

$$C_{2,1}(0,x'_l) = C_2^0,\ C_3(0,x'_l) = C_3^0 \quad l = L/2 + 1, \ldots, L$$

where C_1^0, C_2^0, and C_3^0 are the initial equilibrium concentrations of total monomer both uncomplexed and complexed with ligand, dimer and unbound ligand, respectively; and R is the initial equilibrium ratio, $R = C_{1,1}(0,x'_l)/C_{1,0}(0,x'_l)$. These quantities constitute computer input data, and the values of the equilibrium constants are calculated therefrom:

$$K_1 = R/C_3^0 \tag{11a}$$

$$K_2 = [C_2^0/(C_1^0)^2][(1 + R)^2/R^2] \tag{11b}$$

The boundary values are

$$C_{1,0}(t_n,0) = C_{1,1}(t_n,0) = C_{2,1}(t_n,0) = C_3(t_n,0) = 0$$

$$C_{1,0}(t_n,x'_L) = C_1^0/(1 + R)$$

$$C_{1,1}(t_n,x'_L) = C_1^0 - C_{1,0}(t_n,x'_L)$$

$$C_{2,1}(t_n,x'_L) = C_2^0$$

$$C_3(t_n,x'_L) = C_3^0$$

The values of $\bar{x}$, Δt, $\Delta x'$, macromolecular concentration and per cent dimerization, and macromolecular transport parameters used in these calculations are the same as for nonmediated dimerization; the treatment of the truncation error is also the same. Unless indicated otherwise the rotor speed is 60,000 rpm. $D_3 = 10^{-5}$ cm^2 sec^{-1}; $R = 9.743 \times 10^{-3}$; and $K_2 = 5.625 \times 10^6$ M^{-1}. The theoretical sedimentation patterns are displayed as plots of $\delta(C_1 + 2C_2)/\delta x'$ *vs.* x', where $C_1 = C_{1,0} + C_{1,1}$ and $C_2 \equiv C_{2,1}$.

Finally, mention should be made of the small error introduced into the calculations by linearization of the rate equations, which approximation assumes that the displacements ($y_{1,0}$, $y_{1,1}$, and y_3) of the concentrations of M, MX, and X from their equilibrium values are small. This will be so for small Δt and sufficiently large k's. Even so, the displacements will increase slightly during each time cycle of calculation thereby giving rise to an error propagated in time. This error is negligible for values of k_4 as small as 2×10^{-3} sec^{-1} since the concentrations of the several species are changed by less than 1% during transport for $\Delta t = 1$ sec. For smaller k_4, however, the

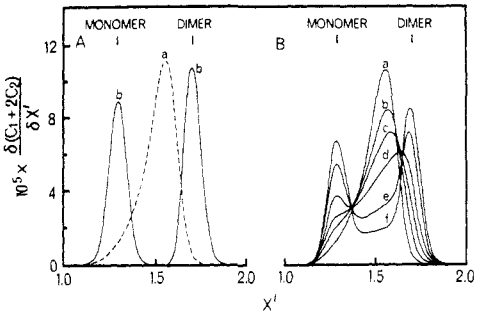

FIGURE 1: Theoretical sedimentation patterns for nonmediated dimerization (reaction I). (A) Sedimentation patterns calculated for the limiting case of instantaneous reestablishment of equilibrium during differential transport of monomer and dimer (curve a) and for the limit in which there is no interconversion during the course of the sedimentation experiment (curve b). (B) Sedimentation patterns for kinetically controlled interaction: a, $k'_2 = 3.6 \times 10^{-2}$ sec^{-1} (half-time, 19 sec); b, 4×10^{-3} sec^{-1}; c, 2×10^{-3} sec^{-1}; d, 10^{-3} sec^{-1}; e, 4×10^{-4} sec^{-1}; and f, 2×10^{-4} sec^{-1} (half-time, 3.5×10^3 sec). Time of sedimentation, 2×10^3 sec. All patterns in this and the following figures are for 52.7% dimerization of the macromolecule.

slow rates of reaction become decisive and cognizance must be taken of the error accrued on the solvent side of the sedimenting boundary over the many time cycles of calculation. The calculation for $k_4 = 10^{-3}$ sec^{-1} was terminated when the displacements at the position of the slower sedimenting peak in the bimodal boundary had reached about 10% of the equilibrium concentrations for M and X and about 25% for MX; and for $k_4 = 10^{-4}$ sec^{-1}, about 20 and 35%, respectively.

Results and Discussion

The implications of kinetically controlled attainment of chemical equilibrium for the sedimentation behavior of dimerizing systems are seen with greatest clarity by first considering the limits of extremely rapid and extremely slow equilibration and then contrasting the results obtained for progressively decreasing rates of reaction with the upper limit of rapid equilibration.

The theoretical sedimentation patterns for nonmediated dimerization (reaction I) are displayed in Figures 1 and 2A. The pattern for instantaneous reestablishment of equilibrium during differential transport of monomer and dimer (curve a in Figure 1A) shows a single, centripetally skewed peak whose apex migrates about 5% faster than the weight-average velocity of monomer and dimer. In the other limit where the rates of reaction are so very slow that virtually no reequilibration occurs during the course of separation of monomer and dimer, the sedimentation pattern (curve b in Figure 1A) shows two peaks aping a mixture of two noninteracting macromolecules. Resolution is complete, the gradient going to the base line between the two well-separated peaks which migrate with the velocity of monomer and dimer; and conventional analysis of the patterns yields the concentration of monomer and dimer in the initial equilibrium mixture.

Instantaneous establishment of equilibrium implies diffusion controlled kinetics ($k'_1 \sim 10^{10}$ sec^{-1} and $k'_2 \sim 10^5$ sec^{-1}) but here we are interested in considerably slower rates of reaction, $k'_1 \sim 4 \times 10^3$ to 20 M^{-1} sec^{-1} and $k'_2 \sim 4 \times 10^{-2}$ to 2×10^{-4} sec^{-1}; *i.e.*, half-times of dissociation of the dimer in the range, 17 to 3.5×10^3 sec, for times of sedimentation of the order of 2×10^3 sec. Comparison of curve a in Figure 1B with curve a in Figure 1A shows that for a half-time of reaction of 19 sec the sedimentation pattern is virtually the same

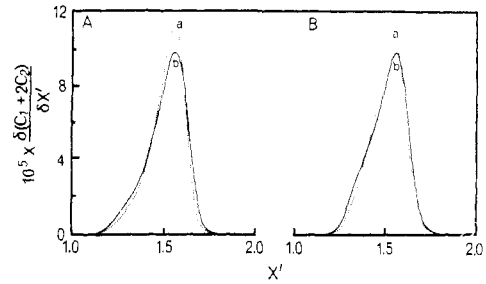

FIGURE 2: Comparison of theoretical sedimentation patterns for instantaneous reequilibration (curve a) and for kinetically controlled interaction with a half-time of dissociation of the dimer of 58 sec (curve b). (A) Nonmediated dimerization (reaction I): for kinetically controlled interaction $k'_2 = 1.2 \times 10^{-2}$ sec^{-1}; time of sedimentation, 2×10^3 sec. (B) Ligand-mediated dimerization (reaction set II): for kinetically controlled interaction, $k_4 = 1.2 \times 10^{-2}$ sec^{-1}; $C_3^0 = 2 \times 10^{-6}$ M; time of sedimentation, 1.5×10^3 sec.

as the pattern obtained for instantaneous reequilibration. Indeed, as illustrated in Figure 2A, in practice it would probably be impossible to distinguish between the patterns for a half-time as long as 60 sec and for instantaneous reequilibration. But, as the half-time is increased further, resolution ensues (Figure 1B). Thus, for a half-time of 347 sec (curve c) the pattern shows a strong, centripetal shoulder; and for a half-time of 693 sec (curve d) the pattern is distinctly bimodal. The sharply defined slower peak migrates with the velocity of the monomer while the broad and centripetally skewed faster one migrates rather slower than the dimer. Increasing the half-time still further enhances the resolution: the slower peak grows in area as the faster one sharpens and drifts toward the velocity of the dimer. Concomitantly, there is evidence of the third peak of intermediate velocity predicted previously for certain range of parameters (Belford and Belford, 1963; Oberhauser *et al.*, 1965); and it is apparent that the gradient will go to the base line between the two major peaks only when the half-time of reaction is manyfold greater than the time of sedimentation. Thus, the family of curves presented in Figure 1 traces the continuous transformation in the shape of the sedimentation pattern from the unimodal one in the limit of instantaneous reequilibration to the completely resolved bimodal one in the limit where a negligible amount of reaction occurs during the course of the sedimentation experiment.

Turning our attention to ligand-mediated dimerization (reaction set II) we note that the shape of the sedimentation pattern for instantaneous reequilibration (Figure 3A) depends upon the initial concentration of unbound ligand, C_3^0. For sufficiently low C_3^0 (*i.e.*, sufficiently strong ligand binding; see eq 11a) the pattern is well resolved into two peaks, but the gradient never goes to the base line between the peaks. Resolution of the pattern depends upon the production and maintenance of concentration gradients of unbound ligand along the centrifuge column by reequilibration during differential transport of the macromolecular species; and the peaks correspond to different equilibrium mixtures and not simply to monomer and dimer. [See Cann (1973) for a physical explanation of the resolution of bimodal reaction boundaries.] Increasing C_3^0 while holding R and the percent dimerization constant (see eq 11a and 11b) causes progressive loss of resolution until at the highest value of C_3^0 the pattern shows a single peak whose shape approaches that shown by nonmediated dimerization when reequilibration is instantaneous (curve a in Figure 1A). In the limit of high C_3^0 the concentration of unbound ligand along the centrifuge column is not significantly perturbed by

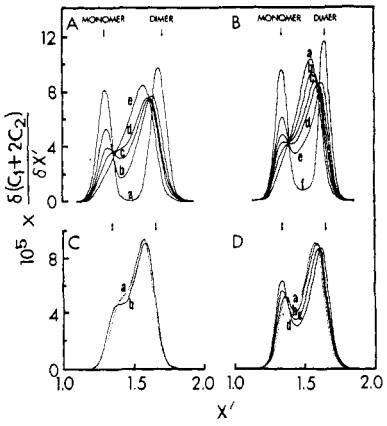

FIGURE 3: Theoretical sedimentation patterns for ligand-mediated dimerization (reaction set II). (A) Instantaneous reequilibration during differential transport of the several species: a, $C_3^0 = 10^{-7}$ M; b, 5×10^{-7} M; c, 7.5×10^{-7} M; d, 10^{-6} M; and e, 2×10^{-6} M. Time of sedimentation, 2×10^3 sec. (B) Kinetically controlled interaction for $C_3^0 = 2 \times 10^{-6}$ M: a, $k_4 = 3.6 \times 10^{-2}$ sec^{-1} (half-time, 19 sec); b, 6×10^{-3} sec^{-1}; c, 3×10^{-3} sec^{-1}; d, 2×10^{-3} sec^{-1}; e, 10^{-3} sec^{-1}; and f, 10^{-4} sec^{-1} (half-time, 6.9×10^3 sec). Time of sedimentation, 1.5×10^3 sec. (C) Comparison of the pattern for instantaneous reequilibration (curve a) with the pattern for kinetically controlled interaction with $k_4 = 1.2 \times 10^{-2}$ sec^{-1}, *i.e.*, half-time of 58 sec (curve b); $C_3^0 = 10^{-6}$ M; time of sedimentation, 1.5×10^3 sec. (D) Comparison of rapidly equilibrating and kinetically controlled interactions for $C_3^0 = 7.5 \times 10^{-7}$ M: a, instantaneous reequilibration; b, $k_4 = 1.2 \times 10^{-2}$ sec^{-1}; c, 3×10^{-3} sec^{-1}; and d, 1.5×10^{-3} sec^{-1}. Time of sedimentation, 1.5×10^3 sec.

the reaction during differential transport so that the system in effect behaves like the nonmediated reaction.

Sedimentation patterns for kinetically controlled ligand-mediated dimerization have been calculated for several values of C_3^0 at fixed $k_2 = 10^4$ sec^{-1} with k_1 ranging from 5×10^7 to 1.3×10^8 M^{-1} sec^{-1} depending upon C_3^0 (see eq 11a and recall that $k_1 = k_2K_1$). These values of the rate constants fall in the upper range of values observed for binding of small molecules by macromolecules[3] (Table II in Havsteen, 1969). The values of k_3 and k_4 have been systematically varied over the range $k_3 \sim 2 \times 10^5$ to 6×10^2 M^{-1} sec^{-1} and $k_4 \sim 4 \times 10^{-2}$ to 10^{-4} sec^{-1}; *i.e.*, half-times of dissociation of the dimer in the range, $\sim$19 to 7×10^3 sec for time of sedimentation, 1.5×10^3 sec.

Let us first consider the effect of chemical kinetics on the shape of the sedimentation pattern for $C_3^0 = 2 \times 10^{-6}$ M, at which concentration of ligand the pattern is unimodal for instantaneous reequilibration. As illustrated by the family of patterns displayed in Figures 2B and 3B, progressively decreasing the rates of macromolecular association and dissociation (*i.e.*, k_3 and k_4) causes essentially the same transformation in the shape of the pattern as observed in the case of nonmediated dimerization. Thus, the pattern for a half-time of dissociation equal to 19 sec is almost indistinguishable from the pattern for instantaneous reequilibration (compare curves a in Figures 2B and 3B); and even though a half-time of about 60 sec distorts the shape of the peak significantly (Figure 2B), it is possible that in practice such a pattern might be misinterpreted as indicative of very rapid equilibration. Upon further increase in the half-time of reaction (Figure 3B)

[3] An exploratory calculation for $C_3^0 = 2 \times 10^{-6}$ M, $k_3 = 6.75 \times 10^4$ M^{-1} sec^{-1}, and $k_4 = 1.2 \times 10^{-2}$ sec^{-1} gave virtually the same sedimentation pattern for $k_1 = 4.87 \times 10^5$ M^{-1} sec^{-1} and $k_2 = 10^2$ sec^{-1} as for $k_1 = 4.87 \times 10^7$ M^{-1} sec^{-1} and $k_2 = 10^4$ sec^{-1}. This result follows from the fact that in both instances the ligand-binding reaction IIa equilibrates much more rapidly than the dimerization reaction IIb.

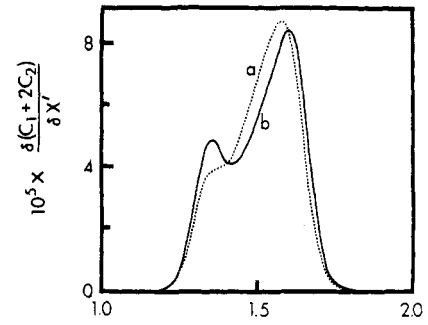

FIGURE 4: Comparison of the sedimentation patterns for kinetically controlled, nonmediated, and ligand-mediated dimerization with the half-time for dissociation of the dimer, 347 sec, being the same in both cases: curve a, nonmediated interaction with $k'_2 = 2 \times 10^{-3}$ sec^{-1}; curve b, ligand-mediated interaction with $C_3^0 = 2 \times 10^{-6}$ M and $k_4 = 2 \times 10^{-3}$ sec^{-1}. Time of sedimentation, 1.5×10^3 sec.

resolution into two peaks ensues and becomes increasingly sharp as the limit is approached wherein negligible interconversion occurs during the course of sedimentation. It is noteworthy that the limit is approached asymptotically, and that even for a half-time fivefold greater than the time of sedimentation (curve f) the gradient still does not go to the baseline between the well-separated peaks. These similarities to nonmediated dimerization are striking. There are differences, however. In particular, cooperation between the transport of ligand and the rate of formation of dimer acts to enhance resolution in the case of the ligand-mediated interaction which, as illustrated in Figure 4, is as a consequence more sensitive to kinetic control.

We have also explored the effect of rotor speed on the shape of the pattern for long half-time of dissociation of dimer. As shown in Figure 5A decreasing the rotor speed broadens the reaction boundary and elevates the gradient between the two peaks. The control calculation presented in Figure 5B indicates that to a large extent this is due to the greater amount of reaction that can occur during the longer time of sedimentation at lower speeds. Although this is undoubtedly a governing factor, there is nevertheless a certain ambiguity here since rapidly equilibrating systems show a similar effect related to the maintenance against diffusion of the concentration gradients of unbound ligand along the centrifuge cell (Figure 81 on p 198 in Cann, 1970).

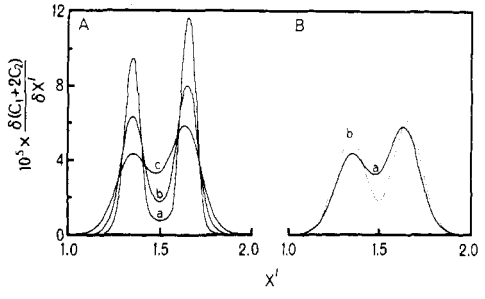

FIGURE 5: Effect of rotor speed on the shape of the sedimentation pattern for kinetically controlled, ligand-mediated dimerization with $C_3^0 = 2 \times 10^{-6}$ M and $k_4 = 10^{-4}$ sec^{-1} (half-time, 6.9×10^3 sec). (A) Family of patterns calculated for different rotor speeds maintaining constant distance of migration, $s_i\omega^2\bar{x}t$: curve a, 60,000 rpm and $t = 1.5 \times 10^3$ sec; curve b, 42,426 rpm and 3×10^3 sec; curve c, 30,000 rpm and 6×10^3 sec. (B) Control calculation to evaluate the effect of increased diffusion of macromolecule on the shape of the pattern at low rotor speed: curve a, interacting system; curve b, uncoupled system in which monomer and dimer migrate independently, *i.e.*, no reequilibration by interaction; 30,000 rpm and 6×10^3 sec.

The effect of kinetic control on the shape of the sedimentation pattern for $C_3^0 = 10^{-6}$ M is explored in Figure 3C. For instantaneous reequilibration the pattern is characterized by a broad centripetal shoulder which is accentuated when the half-time for dissociation of the dimer is about 60 sec. At the lower $C_3^0 = 7.5 \times 10^{-7}$ M the pattern for instantaneous reequilibration is marginally but distinctly bimodal. As the rate of dissociation is decreased (Figure 3D), resolution is sharpened.

Although our calculations have been made for a macromonomer with the molecular weight of lobster hemocyanin, the results also apply qualitatively to smaller proteins whose sedimentation behavior will be somewhat less sensitive to kinetic control due to slower sedimentation velocities. In fact, the three patterns (a, b, and c) presented in Figure 5A have an alternative interpretation to the one presented above: they also apply to dimerizing systems in which the sedimentation coefficient of the monomer is 17, 8.5, and 4.25 S, respectively (25, 12.5, or 6.25 S for the dimer), the rotor speed being held constant at 60,000 rpm with the time of sedimentation varying from 1.5×10^3 to 6×10^3 sec. The only reservation, which is actually of little consequence for comparison of the patterns, relates to the fact that the diffusion coefficients of the two macromolecular species are also held constant in this alternative reading of the figure. In this connection it should be noted that preliminary values for the diffusion coefficients of the hexamer (monomer in our notation) and the dodecamer (dimer in our notation) of lobster hemocyanin at 25° in 0.1 M glycine buffer at pH 9.6 are 3.63×10^{-7} and 2.65×10^{-7} cm^2 sec^{-1}, respectively (S. Park-Yim and G. Kegeles, to be published). Of these, the dodecamer value is considerably more reliable, as hexamer cannot be prepared free of contamination by other species. These values are smaller than the mathematically effective diffusion coefficients in our calculations, but here too this difference is a relatively unimportant consideration for the shape of the sedimentation patterns.

The foregoing results admit several generalizations. First, previous conclusions concerning the sedimentation behavior of ligand-mediated interactions in the limit of instantaneous establishment of equilibrium (Cann and Goad, 1965a,b, 1970, 1972; Cann, 1970, 1973) evidently are valid for kinetically controlled interactions characterized by half-times of reaction as long as 20–60 sec, and the same can be said for nonmediated dimerization. In retrospect that might have been anticipated from a recent theoretical treatment of zonal transport of kinetically controlled dissociation of macromolecular complexes (Cann and Oates, 1973). The computed bimodal reaction zones are strikingly similar to those calculated by Bethune and Kegeles (1961) for very rapid equilibration. Mention has already been made of the greater sensitivity of ligand-mediated dimerization to kinetic control than nonmediated dimerization. Of greater importance for the detection and characterization of macromolecular interactions is the finding that for half-times of dissociation of dimer less than about 200 sec, resolution of the reaction boundary into two peaks can occur only if dimerization is ligand mediated. Cognizance must also be taken of the fact that the bimodal pattern for rapid equilibration under conditions of sufficiently strong ligand binding (curve a in Figure 3A) may bear a strong resemblance to both the pattern shown by very slowly reequilibrating ligand-mediated interaction (curve f in Figure 3B) and the pattern for nonmediated dimerization in the limit where negligible interconversion occurs during the course of sedimentation (curve b in Figure 1A). A more general comparison between the various patterns shown in Figures 1 and 3 underscores the interpretative difficulties that may be encountered in practice, and emphasizes the need for analysis of both freshly prepared and aged fractions to see if they run true. Only in this way is it possible to distinguish between interactions and inherent heterogeneity. In addition such fractionation experiments may provide useful information as to the rates of reaction. In the event that the peaks in a suspected reaction boundary happen to be very well separated, it also behooves one to scrutinize the region between the peaks to ascertain whether or not the gradient actually goes to the base line, even going to the pains of using ultraviolet scanning optics.

Thus, the results of this investigation add to our store of fundamental understanding required for unambiguous interpretation of the sedimentation patterns of interacting systems. But, analytical sedimentation alone does not suffice. It is imperative that several independent physicochemical methods be brought to bear in order to establish the exact nature of the interaction; for example, the combined application of Archibald molecular weight determinations and rapid kinetic measurements as practiced in the case of New England lobster hemocyanin (Morimoto and Kegeles, 1971; Tai and Kegeles, 1971; Kegeles and Tai, 1973).

References

Belford, G. G., and Belford, R. L. (1963), *J. Chem. Phys. 37*, 1926.

Bethune, J. L., and Kegeles, G. (1961), *J. Phys. Chem. 65*, 1755.

Cann, J. R. (1970), Interacting Macromolecules. The Theory and Practice of Their Electrophoresis, Ultracentrifugation, and Chromatography, New York, N. Y., Academic Press.

Cann, J. R. (1973), *Biophys. Chem. 1*, 1.

Cann, J. R., and Goad, W. B. (1965a), *J. Biol. Chem. 240*, 148.

Cann, J. R., and Goad, W. B. (1965b), *J. Biol. Chem. 240*, 1162.

Cann, J. R., and Goad, W. B. (1970), *Science 170*, 441.

Cann, J. R., and Goad, W. B. (1972), *Arch. Biochem. Biophys. 153*, 603.

Cann, J. R., and Oates, D. C. (1973), *Biochemistry 12*, 1112.

Carnahen, B., Luther, H. A., and Wilkes, J. O. (1969), Applied Numerical Methods, New York, N. Y., John Wiley and Sons, Inc., p 319.

Carpenter, D. E., and Van Holde, K. E. (1973), *Biochemistry 12*, 2231.

Eigen, M., and DeMaeyer, L. (1963), *Tech. Org. Chem. 8*, 895.

Ellerton, H. D., Carpenter, D. E., and Van Holde, K. E. (1970), *Biochemistry 9*, 2225.

Gilbert, G. A. (1955), *Discuss. Faraday Soc. 20*, 68.

Gilbert, G. A. (1959), *Proc. Roy. Soc., Ser. A 250*, 377.

Goad, W. B., and Cann, J. R. (1969), *Ann. N. Y. Acad. Sci. 164*, 172.

Havsteen, B. H. (1969), *in* Physical Principles and Techniques of Protein Chemistry, Leach, S. J., Ed., Part A, Chapter 5, New York, N. Y., Academic Press.

Kegeles, G., and Tai, M. (1973), *Biophys. Chem. 1*, 46.

Morimoto, K., and Kegeles, G. (1971), *Arch. Biochem. Biophys. 142*, 247.

Oberhauser, D. F., Bethune, J. L., and Kegeles, G. (1965), *Biochemistry 4*, 1878.

Tai, M., and Kegeles, G. (1971), *Arch. Biochem. Biophys. 142*, 258.